Adaptive Contrast Enhancement of Satellite Images Based on Histogram and Non-linear Transfer Function Methods

Zamfirdaus Saberi*, Noramiza Hashim, Aziah Ali, Patrice Boursier, Junaidi Abdullah and Zarina Che Embi

Abstract— **Satellite images are widely used in various fields as they are important, especially in monitoring activities. Change detection is one such activity that assesses differences in satellite images over time. However, weather and environmental effects may degrade the quality of images. Therefore, the image quality needs to be enhanced before processing the image. This study examined a number of adaptive contrast enhancement approaches based on histogram & non-linear transfer functions, as well as the impact of adopting multiple colour spaces for enhancement. We proposed an enhancement method where the L channel in the CIE LAB colour space was enhanced through a combination of the adaptive gamma correction method with weighting distribution (AGCWD) and Contrast Limited Adaptive Histogram Equalisation (CLAHE). We also advocated using average ranking to select the best method by averaging the various metrics. Improving the performance of change detection, our technique produced the highest average rank of BRISQUE and RMSE contrast values compared to the other methods.**

Index Terms — **contrast enhancement, satellite images, gamma correction, histogram equalisation, change detection**

I. INTRODUCTION

Change detection is a method of assessing differences in a matter's or aspect's state across time [1]. The goal is to determine whether a change has occurred along with the timestamp of any such changes. Multi-temporal satellite data, such as aerial and satellite images, can be used to identify changes in land use and land cover (LULC) across time at a specific location [2]. With the rapid advancement of technology, high resolution remote sensing images can be retrieved for any form of analysis [3]. Differentiating LULC is crucial for a variety of applications, including urban development and monitoring.

Zamfirdaus Saberi is an undergraduate student in Bachelor of Computer Science (Hons) majoring in Data Science at Multimedia University, Malaysia (email: mohdzamfirdaus99@gmail.com).

Noramiza Hashim is a lecturer at Multimedia University, Malaysia (email: noramiza.hashim@mmu.edu.my).

Aziah Ali is a lecturer at Multimedia University, Malaysia (email: aziah.ali@mmu.edu.my).

Patrice Boursier is a lecturer at International Medical University, Malaysia (email: patrice.boursier@imu.edu.my).

Junaidi Abdullah is a lecturer at Multimedia University, Malaysia (email: junaidi.abdullah@mmu.edu.my).

Zarina Che Embi is a lecturer at Multimedia University, Malaysia (email: zarina.embi@mmu.edu.my).

Change detection, which entails identifying differences between two images, is a frequently used application of remote sensing data where the images were captured at different time points. The changes that are discovered will generate a change map identifying the areas that have changed and those that have not. Change detection in multitemporal satellite images can be accomplished via deep learning, in which a convolutional neural network is utilised to train the model for change detection [1][4].

Nevertheless, the ability of satellites is limited in acquiring satellite images due to weather and environmental factors [5]. Poor image quality in satellite images is caused by a number of factors, including non-uniform illumination, a fast shutter cycle, insufficient image sensors, as well as low illumination [6]. Images captured in these conditions have low intensity, fading colours, and contrast distortions. Low-light photos frequently have a small dynamic range, little contrast, and a lot of noise [7]. Hence, image enhancement is regarded as a critical phase of change detection as it ensures the accuracy of the following phases, including the generation of the change map. The purpose of image enhancement is to bring out the features that are normally obscured in a low contrast image [8].

Based on the change detection method, image preprocessing or enhancement takes place before the change detection algorithm because it is necessary to ensure the performance of the change detection by improving the images affected by air disturbances and other noise [6].

A. Image Enhancement Techniques

The techniques for image enhancement can be split into three categories (Figure 2), namely frequency domain, non-linear transfer function-based, with histogram-based [9]. For simple frequency-domain image restoration, the Fourier transform of the visual is calculated, the result is multiplied by a filter, and finally the inverse transformation is carried out. whereas non-linear functions that alter the pixel values directly includes gamma correction as well as logarithmic mapping. Due to their ease of adjustment and application, they are commonly carried out to improve contrast and brightness. Gamma correction has emerged as the most often used nonlinear transfer function in recent years because it accurately mimics the characteristics of the human sensory systems. By changing the digital values

of gloomy photographs, it improves their aesthetics. In contrast, histogram-based methods are frequently employed to balance the grey level distributions in an image [10].

In histogram-based techniques, histogram equalisation (HE) is a straightforward and efficient enhancement technique. HE balances the intensity levels of the input histogram evenly over the full range. Several HE drawbacks include over-enhancement and intensity saturation [11]. Adaptive Histogram Equalisation (AHE) can be used to address these flaws [12], An image is divided into sub-tiles, the combined distribution function (CDF) for every tile is built, and then pixels are overlaid using the cumulative distribution of four nearby tiles. Nonetheless, when the slope of the histogram is severe, noise will inevitably grow. Contrast Limited Adaptive Histogram Equalization (CLAHE) was proposed as a solution to this issue in AHE [13]. After a histogram is generated in CLAHE, it is trimmed using a predetermined threshold and then redistributed among the histogram's pixels. The pixels are then transformed to CDF. As clipping inhibits the CDF from getting steep, it can minimise noise since it stops the CDF from becoming steep [9]. Numerous research has utilised CLAHE to improve image contrast. For images with little illumination, CLAHE may provide high-quality visuals, but its performance in dark places may deteriorate [9]. The scientists claimed that maintaining details while increasing overall brightness is the fundamental to improving low-light images. Integrating nonlinear function with histogram modification to improve intensity while enhancing local contrast is therefore a potential technique.

A nonlinear transfer function, like the gamma correction method, is employed to improve image quality by adjusting contrast while maintaining the average luminance [11]. Determining gamma correction settings manually is a time-consuming process. To improve the image's contrast, an adaptive gamma correction (AGC) approach was presented in which the optimal gamma level is calculated automatically based on the information retrieved from the image [14]. In addition, adaptive gamma correction with weighting distribution (AGCWD), an enhanced variant of AGC, was implemented. It determines the gamma value depends on the CDF of the source images.

B. Colour Space

Other than image enhancement methods, colour space also plays an important role in enhancement. According to Sovdat et al. [15], the axes of the CIE XYZ and RGB colour spaces are not perfectly aligned with the visible qualities of the colour, such as brightness and saturation. So, when simple contrast and chromaticity adjustments are applied, the hue and saturation of the colour will also be changed. Hence, the information in the image cannot be entirely preserved. Therefore, CIELAB (also known as CIE LAB, and CIE L*a*b) colour spaces, which are independent of these features, are preferable alternatives for such adjustments.

C. Overview of the Proposed Method

In light of the description above, an effective technique for picture enhancement was suggested to boost contrast without sacrificing the image's naturalness or information. RGB input image was transformed into the CIELAB colour space in the proposed method before the L channel was enhanced. Combining histogram-based and non-linear transfer function-based techniques, such as AGCWD and CLAHE, it reduces excessive amplification and intensity overload effects to significantly improve contrast. After being converted from the CIELAB colour system to the RGB colour space, an updated and newer image can be produced.

II. PROPOSED METHOD

Based on the methodologies outlined above, this study suggested a technique for effectively enhancing the contrast of satellite images. Figure 1 demonstrates the framework of the proposed method. The proposed enhancement began with colour space conversion, in which the RGB satellite image input was converted to CIELAB colour space. Then, to enhance the contrast of the image while keeping the A and B channels, the histogram-based as well as non-linear transfer-based enhancement techniques, AGCWD and CLAHE were applied to the L channel. Finally, the enhanced CIELAB image was transformed into RGB colour space.

A. RGB to CIELAB Color Space Conversion

The conversion of RGB to CIELAB colour space was done indirectly, using XYZ colour space as an intermediate mode. The LAB colour components are given by the following formula:
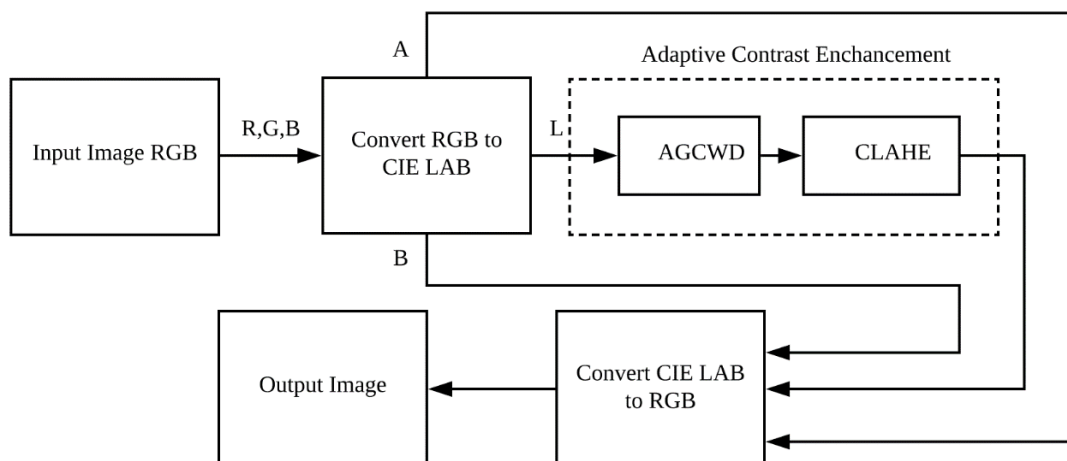

Figure 1. Framework of the proposed method

$$L* = 116 \cdot h\left(\frac{Y}{Y_W}\right) - 16 \qquad (1)$$

$$a* = 500[h\left(\frac{X}{X_W}\right) - h\left(\frac{Y}{Y_W}\right)] \qquad (2)$$

$$b* = 500[h\left(\frac{Y}{Z_W}\right) - h\left(\frac{Z}{Z_W}\right)] \qquad (3)$$

where

$$h(q) = \begin{cases} \sqrt[3]{q} & q > 0.008856 \\ 7.787q + \dfrac{16}{116} & q \leq 0.008856 \end{cases} \qquad (4)$$

and X_W, Y_W, and Z_W are white tristimulus reference values, which are the whites of a perfectly reflecting diffuser under the CIE standards of D65 illumination. Following the colour space conversion, the image was enhanced using CLAHE and AGCWD by conserving the A and B channel components while improving the L channel.

B. Contrast Enhancement Method

AGCWD and CLAHE were utilised to enhance the quality of the L channel in the CIELAB satellite image. The adaptive gamma adjustment for the AGCWD technique was developed using:

$$T(l) = l_{max}(l/l_{max})^\gamma = lmax(l/lmax)^{1-cdf(l)} \qquad (5)$$

Additionally, the statistical histogram was slightly modified and the likelihood of adverse outcomes was decreased by using the weighted distribution (WD) function. The following is how the WD function was created:

$$pdf_w(l) = pdf_{max}\left(\frac{pdf(l) - Pdf_{min}}{Pdf_{max} - Pdf_{min}}\right)^a \qquad (6)$$

where a denotes the gamma value adjustment parameter and pdf denotes the likelihood density function., with pdf_{max} as the maximum pdf of the statistical histogram and pdf_{min} as the minimum pdf. The modified cumulative distribution function (cdf) was defined as:

$$\sum pdf_w = \sum_{l=0}^{lmax} pdf_w(l) \qquad (8)$$

Finally, the gamma parameter relying on cdf for formula $T(l)$ was calculated using the following equation:

$$\gamma = l - cdf_w(l) \qquad (9)$$

In order to remove the maximum values from the histograms for each block, CLAHE limits the contrast by a clipping point, which sets it apart from standard HE. The clipped pixels are distributed among each grey range. The following formula was employed to determine the clipping point:

$$\beta = \frac{M}{N}(1 + \alpha\, 100\, Smax) \qquad (10)$$

The variables M, N, Smax, and α relate to the number of pixels in each frame, the dynamic gamut of the block, the highest slope, and the clipping factor, which, when set to 0, causes the clip point to be M/N, which results in a constant pixel in this block. The difference becomes much more pronounced when the value gets closer to 100. The clipping point is thus the most crucial element in determining the image contrast. To reconfigure the image blocks' grey levels, we obtained a transformation matrix based on CDF as shown in:

$$cdf(l) = \sum_{k=0}^{L} pdf(l) \qquad (11)$$

$$T(l) = cdf(l) \times l_{max} \qquad (12)$$

The remapping function $T(l)$, the pixel grey level l, and the block's highest pixel value l_{max} are specified. On the basis of the CDF of the reallocated histogram in every block, distinct rebinding algorithms were developed. To avoid blocking artefacts, each pixel value was extrapolated from the adaptive thresholding in the neighboring blocks. The four blocks' central pixels are designated as points a, b, c, and d, while the outermost pixel, p, is chosen at random. The rebind pixel p was calculated using the linear transformation as regards:

$$\begin{aligned} T(p(i)) &= m \cdot (n \cdot T_a \cdot p(i) + (1-n) \cdot T_b \cdot p(i))) \\ &+ (1-m) \cdot (n \cdot T_c \cdot p(i) + (1-n) \cdot T_d \cdot p(i)) \end{aligned} \qquad (13)$$

$$\begin{cases} n = (x_b - x_p)(x_b - x_a) \\ m = (y_c - y_p)(y_c - y_a) \end{cases} \qquad (14)$$

The rebinding method is denoted by T(.), and the value of randomized pixel I with dimensions is denoted by p(i) (x, y). Finally, the processed intensity of the image in channel L was merged with the A and B colour components before being converted into the RGB colour space to obtain the improved image.

III. EXPERIMENTAL SETUP

In RGB colour space, the recommended method was compared to the histogram as well as non-linear transfer function optimization techniques. The proposed approach was contrasted with one that makes use of histograms and non-linear model parameters in various colour spaces.

Then, the proposed method was evaluated and applied to build deep learning-based change detection for multitemporal satellite images. Once the dataset for the training change detection model was enhanced, the proposed technique was used in image pre-processing. Finally, the trained change detection model was compared to the non-enhanced model to determine the influence of performance enhancements on the change detection model.

A. Satellite Images Sample

500 satellite images of varying brightness and contrast were used to test the enhancement methods. A portion of the images was hazy and misty. The Semantic Change Detection Dataset's images were selected at random (SECOND) [16]. These collections of aerial imagery also include those from Shanghai, Chengdu, and Hangzhou. The images were captured using a variety of platforms and sensors.

B. Image Quality Assessments

The proposed approach was evaluated utilizing Root Mean Square Error (RMSE) of contrast, the Blind/Referenceless Image Spatial Quality Evaluator (BRISQUE) assessment, as well as the average score.

RMSE performance measure was used since this study employed a histogram-based method that tends to over-enhance. By contrasting the increased output with the corresponding manually enhanced ground-truth images, the estimator can identify the image's contrast inconsistency. Following are the steps to calculate the RMSE:

$$RMSE = \sqrt{\frac{\sum_{i=1}^{N} ||y(i) - \hat{y}(i)|^2}{N}} \qquad (15)$$

N stands for the number of points, y(i) for the measurements at position I and $y(i)$ for such forecast at position i.

On the other hand, the output image generated from each enhancement method was also evaluated by the Blind/Referenceless Image Spatial Quality Evaluator (BRISQUE). BRISQUE is a referenceless quality assessment technique. It is, to some extent, a holistic evaluation metric that leverages "natural scene statistics" to quantify the absence of "naturalness" in an image and the presence of distortions [17]. The value of the BRISQUE score ranges from 0 to 100, with lower values indicating higher quality output images.

Since RMSE and BRISQUE, two distinct evaluation criteria, were utilised in this study to evaluate the enhancement method, the average ranking was employed to decide which enhancement approach was optimal. Prior to averaging, the RMSE of the contrast and the BRISQUE score are ranked individually.

$$Average\ rank = \frac{RMSE\ rank + BRISQUE\ rank}{2} \qquad (16)$$

C. Change Detection Model Building

After analysing the enhancement techniques and proposed method, the proposed enhancement method was used in the pre-processing stage of the change detection method to examine the influence of the enhancement on the performance of the deep learning-trained change detection model. To perform the comparison, two change detection models were trained; one with enhancement and another one without enhancement. The outputs from both models were then analysed and discussed.

IV. RESULT AND DISCUSSION

A. Quality Assessment of Enhanced Images in Single Method

Other non-linear transition function-based as well as histogram-based approaches on RGB colour space were contrasted with the suggested combination we developed (CLAHE and AGCWD). This comparison was made to assess the effects of a combination method vs. a single method.

In RGB colour space, Table I summarises the outcomes of the improvement approaches that rely on the histogram as well as non-linear transfer function as well as our suggested combination methodology. The RGB colour space is maintained as a constant variable.

Figure 2 visualises the results from Table I in the form of a bar chart ranked from the top to the lowest based on average ranking (left to right). Based on the chart, the proposed combination of AGCWD and CLAHE achieved acceptable average scores for BRISQUE and RMSE of contrast (the smaller the two matrices, the better the result). The suggested combination strategy, which has a slightly bigger contrast error and a higher BRISQUE score than CLAHE, came in second with regard to average rank value. While, the HE method achieved the highest BRISQUE score of 18.676, but suffered from a high contrast RMSE of 27.687 as depicted in Figure 4(i). AHE had the lowest RMSE contrast and the lowest BRISQUE score (21.993), but it also had the best RMSE contrast and the lowest error.

B. Quality Assessment of Enhanced Images in Different Color Spaces

We also assessed and compared our combination technique (AGCWD and CLAHE) to other colour spaces and the suggested colour space, CIELAB. Table II (visualised in Figure 3) summarises the results of an experiment in which the proposed combination method was evaluated using various colour spaces and compared to the recommended colour space, CIELAB.

TABLE I
COMPARISON OF PROPOSED COMBINATION METHOD WITH OTHER SINGLE METHODS IN RGB

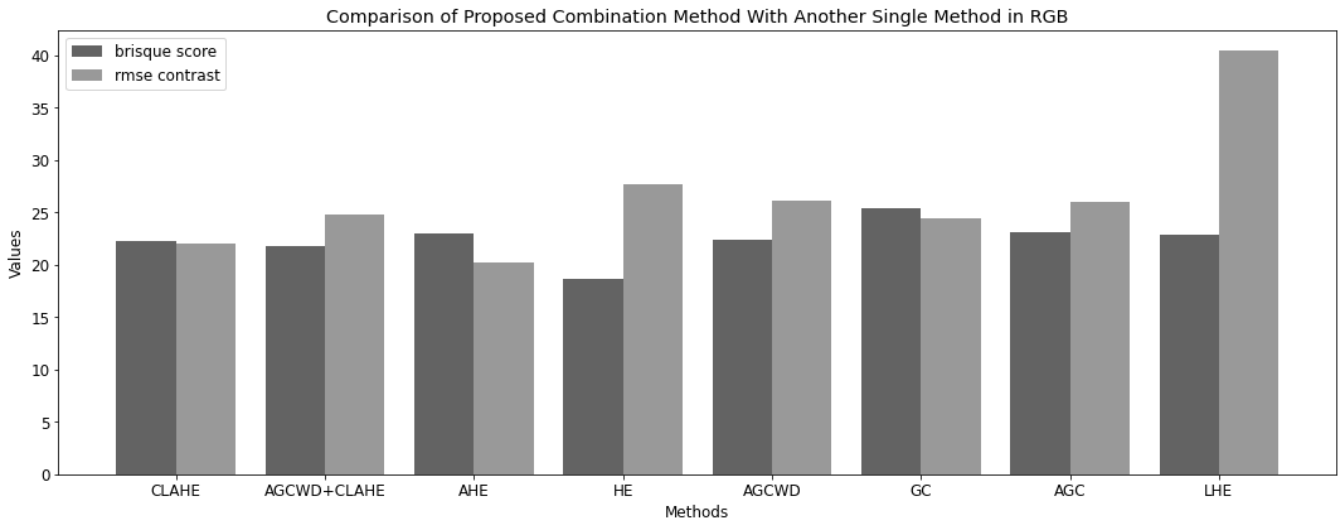| Color Space	Method	Mean BRISQUE Score	RMSE	Rank BRISQUE	Rank RMSE	Average Rank
RGB	LHE	22.842	40.386	5.0	8.0	6.5
RGB	HE	18.676	27.687	1.0	7.0	4.0
RGB	CLAHE	22.208	22.025	3.0	2.0	2.5
RGB	AHE	22.993	20.195	6.0	1.0	3.5
RGB	GC	25.352	24.428	8.0	4.0	6.0
RGB	AGCWD	22.401	26.167	4.0	6.0	5.0
RGB	AGC	23.044	26.000	7.0	5.0	6.0
RGB	AGCWD + CLAHE	21.801	22.986	2.0	3.0	2.5

Figure 2. Bar Graph Comparison of Proposed Combination Method with Another Single Method in RGB
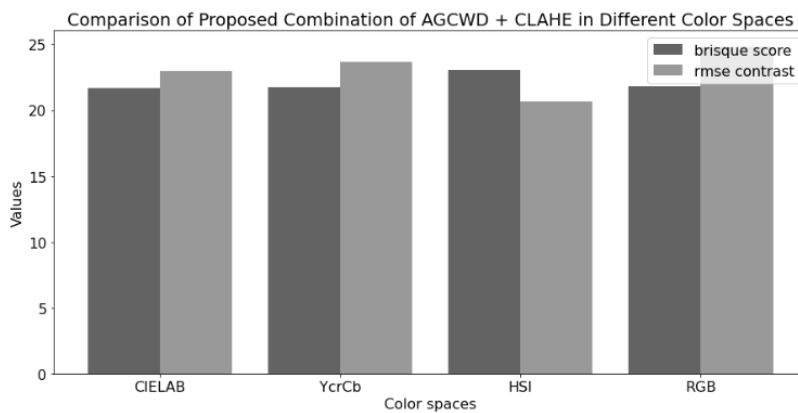

Figure 3. Bar Graph Comparison of the Proposed Combination of AGCWD + CLAHE in Different Color Spaces

The method proposed consists of combination between AGCWD with CLAHE. Clip limit is a numeric value that determines the amount of noise amplified. Upon calculating the histogram for each sub-area, they were redistributed to ensure that their height did not exceed the specified clip limit.

As demonstrated in Table II and Figure 5, our proposed technique (AGCWD and CLAHE in CIELAB colour space) achieved the highest average rank of 1.5. It achieved a reasonable average between the BRISQUE score and the contrast RMSE. Although the HSI colour space had the strongest RMSE contrast with only an error of 20,675, it also had the highest BRISQUE score, signifying a poor image quality. In short, the proposed method outperformed previous methods and colour spaces based on the histograms and non-linear transfer functions.

Figure 5 illustrates a comparison of the enhanced images obtained using the methods described in Table II. Overall, it was clear from visual inspection that the suggested solution (Figure 5(b)) kept the image's natural appearance while removing some foggy clouds to boost contrast. Additionally, it can improve the picture without distorting the colours.

C. Enhancement Effects on Change Detection Model

To train the model, the Unet architecture was adopted. The LEVIR dataset was implemented into the architecture as supervised learning. To train the model, the same hyperparameter setting was used to train both the enhanced and non-enhanced models. Table III lists the details of the hyperparameter setting.

TABLE II
COMPARISON OF COMBINATION OF AGCWD + CLAHE IN DIFFERENT COLOR SPACES

Color Space	Mean BRISQUE Score	RMSE of Contrast	Rank BRISQUE	Rank RMSE of Contrast	Average Rank
CIELAB[1]	21.656	22.986	1	2	1.5
YCbCr	21.774	23.655	2	3	2.5
RGB	21.801	24.800	3	4	3.5
HSI	23.066	20.675	4	1	2.5

[1] Proposed method

(a) input	(b) GC	(c) AGCWD+CLAHE	(d) AGC	(e) AGCWD

(f) AHE	(g) CLAHE	(h) LHE	(i) HE
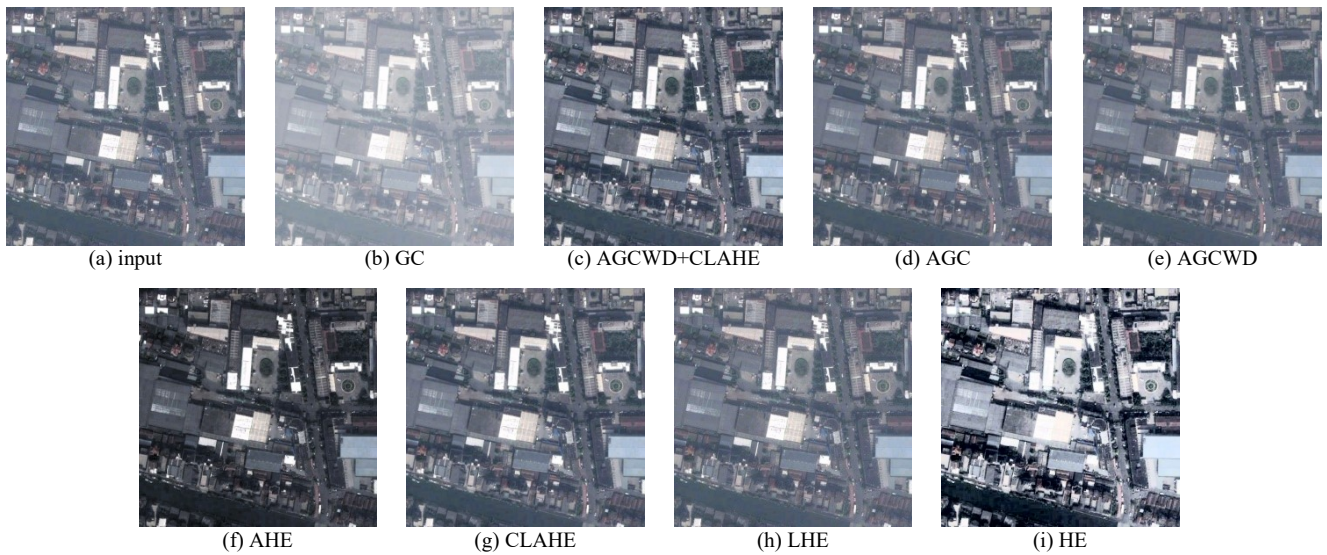
Figure 4. Examples of an individual method's improvement outcomes using the RGB colour space

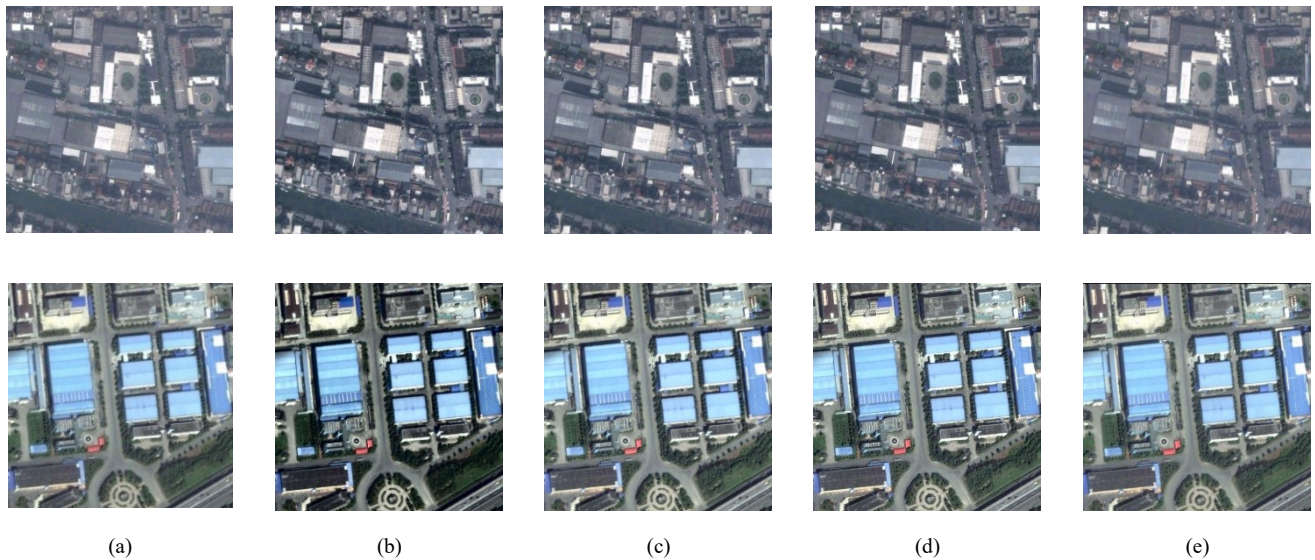| (a)	(b)	(c)	(d)	(e)

Figure 5. Examples of enhancement result based on combination of AGCWD+CLAHE in different color spaces (a) Input images; (b) CIELAB; (c) YCbCr; (d) RGB; (e) HSI;

TABLE III
HYPERPARAMATER SETTING FOR MODEL TRAINING

Network architecture	Unet
Network total parameters	1,941,537
Learning rate	0.001
Batch size	8
Epoch	20
Optimizer	Adam

The training model's findings are shown in Table IV. The LEVIR dataset was initially improved for the enhanced model using the suggested enhancement technique. As for the non-enhanced model, the dataset was used directly for the training model.

As depicted in Table IV, the enhanced model obtained a higher overall result compared to the non-enhanced models. The accuracy of the enhanced model was greater than that of the non-enhanced models, indicating the accuracy of the enhanced model in predicting changes. The enhanced model obtained a higher recall of 0.5510, compared to the non-enhanced model (0.5314). Recall reflects the model's sensitivity. Moreover, the precision for the enhanced model was slightly higher than that of the non-enhanced model, where it yielded 0.5353. Meanwhile, the F1 score which denotes the harmonic mean for recall and precision, indicated that the enhanced model was better. Whereas, for intersection over union (IoU), the enhanced model obtained a higher value of 0.6142 compared to the non-enhanced model, 0.5876. IoU measures the extent to which two boxes, prediction, and ground truth, overlap. The greater the overlap region, the larger the IOU.

TABLE IV
RESULT OF CHANGE DETECTION MODEL TRAINING

Evaluation Metric	Enhanced Model	Non-enhanced Model
Accuracy	0.9718	0.9694
Recall	0.5510	0.5314
Precision	0.5353	0.5092
F1 Score	0.6344	0.5999
Intersection over Union (IoU)	0.6142	0.5876

The graph of training accuracy against validation accuracy over the total number of epochs for enhanced and non-enhanced models is depicted in Figure 6. The accuracy and validation accuracy rise together for the non-enhanced model (Figure 6(b)) indicating that the model trained is not overfitting. The constant line in the graph with a slight increase as it reaches a plateau indicated that the model was unable to learn anymore. As for the enhanced model, the accuracy and validation accuracy lines demonstrated a striking growth indicating that the model can be trained with more epochs to yield a better model with higher performance.

On the other hand, Figure 7 represents training loss vs. validation loss for the non-enhanced and enhanced models. The training loss refers to the fitting of the model with the training data, while the validation loss represents the fit of the model with new data. Based on the loss graphs, the line for training and validation losses were close and decreased with the number of epoch iterations. Hence, both models were not underfitting, as the algorithm captured the training and new data. However, the enhanced model (Figure 7 (b)) indicated a lower loss since the two lines for training and validation were interrelated and dropped uniformly together.

Figure 8 illustrates a pair of multitemporal images (image 1 and image 2) along with their corresponding ground truth of change area and image results of prediction using trained models, i.e., non-enhanced and enhanced. Visually, the enhanced model could predict changes better and detect specific changes in certain areas which explains the higher IoU as it could detect changes along the edges of the building. Whereas, the non-enhanced model can only detect some changes, where some areas of changes are left undetected. Moreover, the non-enhanced model predicted incorrectly where it indicated changes in no change areas.
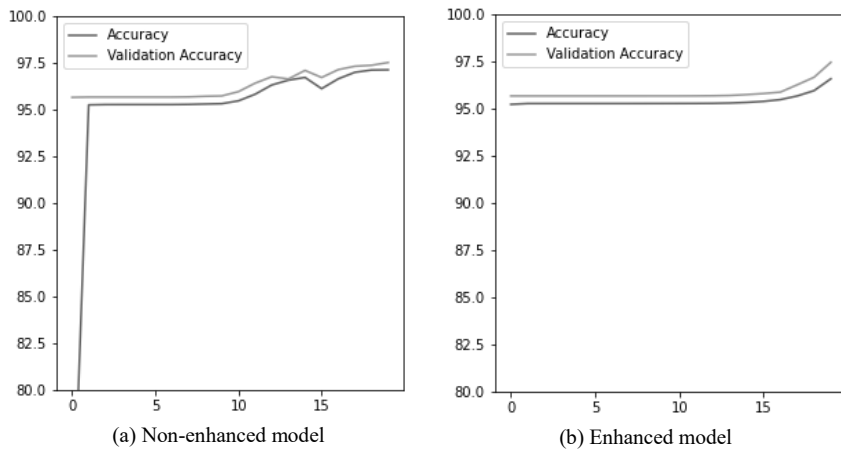

(a) Non-enhanced model   (b) Enhanced model
Figure 6. Accuracy of train and validation learning curves
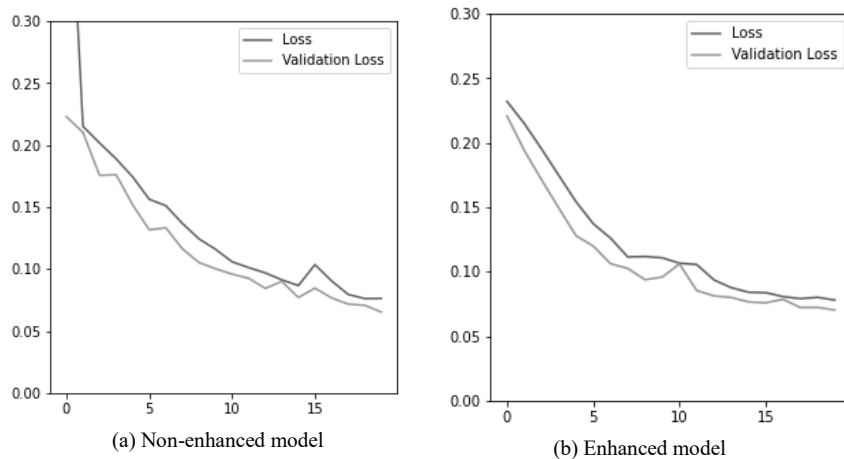
(a) Non-enhanced model   (b) Enhanced model
Figure 7. Loss of train and validation learning curves

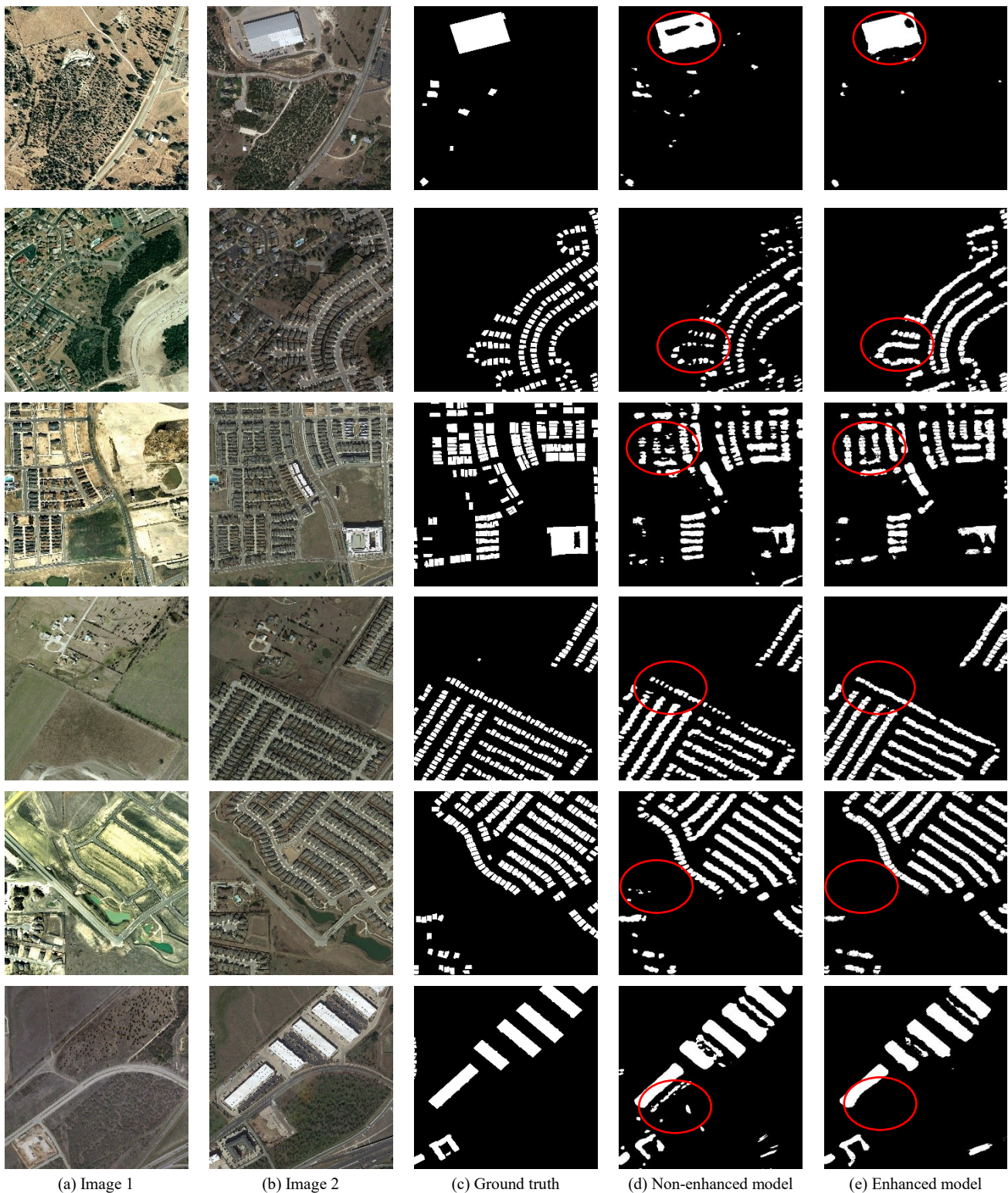| (a) Image 1 | (b) Image 2 | (c) Ground truth | (d) Non-enhanced model | (e) Enhanced model |

Figure 8. Prediction results of trained model on LEVIR-CD dataset

V. CONCLUSION

According to the results, the adaptive contrast enhancement method we presented, which combines CLAHE with AGCWD in the CIELAB colour space, produced the optimal outcomes. It can also be used to improve the performance of change detection activities.

The use of the CIELAB colour space in the proposed method was also supported [15] as CIELAB was accepted as the preferable colour space for image enhancement as it can preserve the information in the image. The results of this investigation are consistent with those of an earlier study [9], which found that using a combined histogram-based as well as non-linear transfer functions method led to superior outcomes with maximum intensity and localized contrasts.

REFERENCES

[1] H. Chen and Z. Shi, "A Spatial-Temporal Attention-Based Method and A New Dataset for Remote Sensing Image Change Detection," Remote Sensing., vol. 12, no. 10, pp1662, 2020

[2] L. Ma, Y. Liu, X. Zhang, Y. Ye, G. Yin, and B. A. Johnson, "Deep Learning in Remote Sensing Applications: A meta-analysis and Review," ISPRS Journal of Photogrammetry and Remote Sensing, vol. 152, no. April, pp166–177, 2019

[3] A. Alzu'bi, A. Amira, and N. Ramzan, "Learning Transfer Using Deep Convolutional Features for Remote Sensing Image Retrieval," IAENG International Journal of Computer Science, vol. 46, no. 4, pp637-644, 2019

[4] A. Hagag, X. Fan, and F. E. A. El-Samie, "Satellite Images Broadcast Based on Wireless Softcast Scheme," IAENG International Journal of Computer Science, vol. 44, no. 1, pp1–7, 2017

[5] M. H. Lee, S. B. Lee, Y. D. Eo, S. W. Kim, J. H. Woo, and S. H. Han, "A Comparative Study on Generating Simulated Landsat NDVI Images Using Data Fusion and Regression Method—The Case of The Korean Peninsula," Environmental Monitoring and Assessment, vol. 189, no. 7, pp333, 2017

[6] K. Lim et al., "Change Detection Based on Artificial Intelligence: State-of-The-Art and Challenges," Remote Sensing, vol. 1, no. 10, pp509–515, 2020

[7] P. Pandey, K. K. Dewangan, and D. K. Dewangan, "Enhancing The Quality of Satellite Images by Preprocessing and Contrast Enhancement" IEEE International Conference on Energy Communication Data Analytics and Soft Computing ICCSP 2017, vol. 2018 January, pp56–60, 2017

[8] X. Zhu, X. Xiao, T. Tjahjadi, Z. Wu, and J. Tang, "Image Enhancement Using Fuzzy Intensity Measure and Adaptive Clipping Histogram Equalization," IAENG International Journal of Computer Science, vol. 46, no. 3, pp395-408, 2019

[9] Y. Chang, C. Jung, P. Ke, H. Song, and J. Hwang, "Automatic Contrast-Limited Adaptive Histogram Equalization with Dual Gamma Correction," IEEE Access, vol. 6, pp11782–11792, 2018

[10] S. K. Swee, L. C. Chen, and T. S. Ching, "Contrast Enhancement in Endoscopic Images Using Fusion Exposure Histogram Equalization," Engineering Letters, vol. 28, no. 3, pp715-723, 2020

[11] M. Veluchamy and B. Subramani, "Image Contrast and Color Enhancement Using Adaptive Gamma Correction and Histogram Equalization," Optik, vol. 183, no. February, pp329–337, 2019

[12] K. Honda, K. Wei, M. Arai, and H. Amano, "CLAHE Implementation on A Low-End FPGA Board by High-Level Synthesis," 2020 Eighth International Symposium on Computing and Networking Workshops (CANDARW), pp282–285, Nov. 2020

[13] C. Wang and B. Zhu, "Image Segmentation and Adaptive Contrast Enhancement for Haze Removal," IEEE 63rd International midwest symposium on circuits and systems, vol. 2020-August, pp1036–1039, 2020

[14] N. M. Hong and N. Chi Thanh, "A Single Image Dehazing Method Based on Adaptive Gamma Correction," 2019 6th NAFOSTED Conference on Information and Computer Science (NICS), pp558–562, 2019

[15] B. Sovdat, M. Kadunc, M. Batič, and G. Milčinski, "Natural Color Representation of Sentinel-2 Data," Remote Sensing Environment, vol. 225, no. September 2017, pp392–402, 2019

[16] A. Varghese et al., "Fully Convolutional Siamese Networks for Change Detection," Proc. 25th IEEE International Conference Image Process. (ICIP), vol. 11130 LNCS, no. 7, pp4063–4067, 2019

[17] K. Ma, W. Liu, T. Liu, Z. Wang, and D. Tao, "DipIQ: Blind Image Quality Assessment by Learning-to-Rank Discriminable Image Pairs," IEEE Trans. Image Process., vol. 26, no. 8, pp3951–3964, 2017